In Vivo Characterization of $^{123/125}$I-2-Iodo-L-Phenylalanine in an R1M Rhabdomyosarcoma Athymic Mouse Model as a Potential Tumor Tracer for SPECT

Veerle Kersemans, MSc[1]; Bart Cornelissen, PhD[1]; Ken Kersemans, MSc[2]; Matthias Bauwens[2]; Erik Achten, PhD[3]; Rudi A. Dierckx, PhD[4]; John Mertens, PhD[2]; and Guido Slegers, PhD[1]

[1]Laboratory for Radiopharmacy, Universiteit Gent, Gent, Belgium; [2]Laboratory for Medical Imaging and Physics, Vrije Universiteit Brussel, Brussels, Belgium; [3]Department of Radiology and Magnetic Resonance Imaging, Gent University Hospital, Gent, Belgium; and [4]Division of Nuclear Medicine, Gent University Hospital, Gent, Belgium

The application of ^{123}I-3-iodo-α-methyltyrosine is limited to diagnosis of brain tumors due to its marked long-term uptake in kidneys. In vitro evaluation of ^{125}I-2-iodo-L-phenylalanine showed high uptake in R1M cells by L-type amino acid transport system 1 (LAT1). This study evaluates ^{123}I-2-iodo-L-phenylalanine as a new specific tumor tracer for SPECT. **Methods:** $^{123/125}$I-2-Iodo-L-phenylalanine is prepared as a one-pot kit using the Cu^{1+}-assisted isotopic exchange method. The characteristics of ^{125}I-2-iodo-L-phenylalanine were examined in vivo in R1M tumor–bearing athymic mice and in acute inflammation–bearing NMRI mice. The uptake of $^{123/125}$I-2-iodo-L-phenylalanine in tumor and other organs of interest was measured by dynamic planar imaging (DPI) and γ-counting after dissection. Displacement of ^{123}I-2-iodo-L-phenylalanine radioactivity by L-phenylalanine, L-methionine, and L-cysteine was measured. ^{123}I-Iodo-human serum albumin planar imaging was performed to correct for blood-pool activity and MRI was performed to delineate the tumor in DPI. ^{18}F-FDG uptake was measured with an animal PET scanner. ^{125}I-2-Iodo-L-phenylalanine and ^{18}F-FDG uptake in inflamed muscle were compared. **Results:** $^{123/125}$I-2-Iodo-L-phenylalanine showed a high and fast tumor uptake and followed a reversible first-order pattern allowing calculation of the half-life and the time to reach equilibrium (t_R). Net tumor-to-background ratios up to 6.7 at 60 min were obtained. This radioactivity was significantly displaced by L-phenylalanine, L-methionine, and L-cysteine, pointing to reversible LAT transport. When plotting t_R of the tumor uptake as a function of tumor volume, a rectangular hyperbolic curve was obtained. The almost constant t_R values at higher tumor volumes (>4 mL) could be linked to increased necrotic tissue. Fast blood clearance of the tracer through the kidneys to the bladder and low tracer activity in the abdomen and brain were observed. The inflamed muscle showed only a slight increase of ^{125}I-2-iodo-L-phenylalanine uptake (inflammation-to-background ratio, RIB = 1.30 ± 0.02), in contrast to the high ^{18}F-FDG uptake (RIB = 11.1 ± 1.7). The in vivo stability of $^{123/125}$I-2-iodo-L-phenylalanine was good: Only 7% of free radioiodide and no other labeled metabolites were observed after 90 min. **Conclusion:** $^{123/125}$I-2-Iodo-L-phenylalanine is quickly taken up by the overexpressed LAT1 system in R1M tumors with high tumor specificity. The availability of a kit and the specificity of the tracer make ^{123}I-2-iodo-L-phenylalanine a promising tool for oncologic SPECT.

Key Words: ^{123}I-2-iodo-L-phenylalanine; radiolabeled amino acids; tumor imaging; inflammation; biodistribution; ^{18}F-FDG

J Nucl Med 2005; 46:532–539

Both amino acid transport across the cell membrane and the protein synthesis rate are early features of malignant transformation. A- and L-type amino acid transport has been shown to be increased in tumor cells relative to normal tissue, and these transport systems have been the major focus of the development of amino acid tumor tracers for oncologic imaging (*1,2*).

At present, ^{123}I-3-iodo-α-methyltyrosine is the only routinely used amino acid tracer for SPECT tumor diagnosis. In comparison with ^{18}F-FDG, this tracer has major advantages, such as high and fast tumor uptake and rather low uptake in gray matter and inflammatory lesions. However, its marked long-term renal accumulation limits its use for oncologic imaging outside the brain (*2–5*). Recently, other L-system–transported radiolabeled amino acids for SPECT have been developed and evaluated to overcome this problem: 2-iodo-L-tyrosine (*6*), 4-iodo-L-phenylalanine (*7*), and 2-iodo-L-phenylalanine. The latter was developed in our research group and showed high accumulation in vitro by L-type amino acid transport (more specifically, LAT1) in R1M (rhabdomyosarcoma) tumor cells without incorporation in the cell proteins (*8*). Recent publications verified that incorporation of radiolabeled amino acids is not necessary and

Received May 5, 2004; revision accepted Nov. 17, 2004.

For correspondence or reprints contact: Veerle Kersemans, MSc, Laboratory of Radiopharmacy, Harelbekestraat 72, B-9000 Gent, Belgium.

E-mail address: veerle.kersemans@ugent.be

that the increased uptake is directly related to the metabolic requirements of the tumor cells (*8*). Therefore, we evaluated in vivo, in the rodent, ^{123}I-2-iodo-L-phenylalanine as a potential SPECT tracer to detect brain as well as peripheral tumors.

MATERIALS AND METHODS

All of the conventional products used were at least analytic or clinical grade and were obtained from Sigma-Aldrich. The solvents were of high-performance liquid chromatography quality (Chemlab).

Synthesis of Precursor 2-I-L-Phenylalanine

2-I-L-Phenylalanine was prepared from 2-Br-L-phenylalanine (PepTech Corp.) using Cu^{1+}-assisted nucleophilic exchange under acidic and reducing conditions (30.3 mmol/L 2-Br-L-phenylalanine, 4.4 mmol/L $CuSO_4$, 8.9 mmol/L citric acid, 9.0 mmol/L $SnSO_4$, 10.7 mmol/L gentisic acid, 44.5 mmol/L NaI) at 160°C for 16 h (*9*). 2-I-L-Phenylalanine and 2-Br-L-phenylalanine were recovered separately from reversed-phase HPLC (RP-HPLC) separation (Hibar Lichrosorb RP-select 7 μm; λ = 261 nm; Merck) with 20:80 MeOH/H_2O containing 1 mmol/L NH_4Ac (pH 5.5, 13 mL/min), and 2-I-L-phenylalanine was purified from methanol by evaporation. Identification and quality control were achieved by NMR, liquid chromatography mass spectroscopy, thin-layer chromatography, and HPLC. Chiral chromatography (5-μm Chirobiotic T, 150 × 4.6 mm; Astec) with 20:80 MeOH/H_2O containing 20 mmol/L NH_4Ac (pH 5.5, 1 mL/min) was used to check chiral modification to 2-I-D-phenylalanine.

Radiochemistry

^{123}I/^{125}I-2-Iodo-L-Phenylalanine. Radioiodination with ^{123}I (222 MBq; 10–20 μL) or ^{125}I (37 MBq; 10 μL) (Nordion Europe) of 1.0 mg 2-I-L-phenylalanine was performed by Cu^{1+}-assisted isotopic exchange (*9*) under acidic and reducing conditions (0.2 mg $CuSO_4$, 2.5 mg citric acid, 0.5 mg $SnSO_4$, 1.3 mg gentisic acid in 565 μL; 60 min at 100°C). The reaction mixture was drawn up in a syringe containing the appropriate amount of 71 mmol/L trisodium citrate dihydrate to render the solution isotonic and to adjust the pH to at least 4. The reaction mixture was filtered through a 0.22-μm Ag filter (Millipore) and a sterile 0.22-μm filter (Millipore) into a sterile vacuum penicillin vial to remove the free $^{123/125}I^-$. Identification and quality control were achieved by HPLC and Sep-Pak C_{18} (Waters). Chiral chromatography was used to check the absence of 2-I-D-phenylalanine.

^{123}I-Iodo-Human Serum Albumin (HSA). Radioiodination of HSA with ^{123}I (Nordion Europe) was performed by electrophilic substitution using the IODO-GEN technique. IODO-GEN (1,3,4,6-tetrachloro-3α,6α-diphenylglycouracil; Pierce) was coated on the wall of polypropylene vials using 70 μg of IODO-GEN per 200 μL of chloroform per vial. The solvent was evaporated by air flow at room temperature. In the IODO-GEN vial, the ^{123}I (111 MBq) solution was added to HSA (50 μg) in 140 μL 0.1 mol/L potassium phosphate buffer at pH 8.5. After 15 min at room temperature, the mixture was removed from the IODO-GEN–coated vial to stop the reaction and was filtered through a 0.22-μm Ag filter to remove the free $^{123}I^-$ from ^{123}I-Iodo-HSA. The specific activity was 1.5 × 10^5 GBq/mmol. Quality control was achieved using a standard prepacked PD-10 SEC column (size-exclusion chromatography; Amersham Pharmacia Biotech) using phosphate-buffered saline/HSA as the eluting agent.

In Vivo Experiments

Laboratory Animals. Water and food were freely available during the experimental period. For the tumor model, male SWISS~*nu/nu* mice (n = 33) (Bioservices) were injected subcutaneously in the right flank (armpit region) with 5 × 10^6 R1M rhabdomyosarcoma cells. Tumors were grown and normal tumor growth curves were obtained using sliding caliper measurement and the estimate volume formula $V = 0.4\ a^2 \cdot b$, with a and b being the short axis and the long axis of the tumor, respectively (*10*). Imaging experiments with ^{123}I-2-iodo-L-phenylalanine, ^{123}I-HSA, and ^{18}F-FDG and dissection experiments with ^{125}I-2-iodo-L-phenylalanine were performed.

For the inflammation model, male NMRI mice (n = 9) (in-house breeding program) were injected in the right biceps brachii with 25 μL of turpentine. Imaging (^{123}I-2-iodo-L-phenylalanine, ^{123}I-HSA, and ^{18}F-FDG) and dissection (^{125}I-2-iodo-L-phenylalanine and ^{18}F-FDG) experiments with the inflamed mice were performed 24 h after turpentine injection.

During all imaging experiments, the animals were anesthetized intraperitoneally with 75 μL (1.5 mg) of solution containing 20 mg pentobarbital per milliliter (Nembutal, 60 mg/mL; Ceva Santé Animale). For the biodistribution experiments by dissection, the animals were killed without sedation by cervical dislocation and the organs of interest were dissected.

All tracers ($^{123/125}$I-2-iodo-L-phenylalanine, ^{18}F-FDG, and ^{123}I-HSA) were injected intravenously in the lateral tail vein. The study protocol was approved by the ethical committee for animal studies of our institution.

Dynamic Planar Imaging (DPI). Imaging was performed using a γ-camera (Toshiba GCA-9300A/hg) in planar mode equipped with a high-resolution, parallel-hole collimator. All images were acquired into 128 × 128 matrices (field of view, 23.5 × 12.46 cm) and with a photopeak window set at 15% around 159 keV. Together with the animals, a syringe with a known amount of radioactivity was scanned, to allow the semiquantification of the results of the region-of-interest (ROI) analysis. The ROIs were drawn using an MRI maximum intensity projection (*10*). The ROI of the heart was used as a measure for blood-pool activity. Due to partial-volume effects, the measured blood-pool data will be overestimated (*11*). The injected dose (ID) was calculated as the amount of radioactivity in the syringe before and after injection (Capintec CRC-15R). The tracer uptake was expressed as the percentage ID per pixel (%ID/P).

At first, an ^{123}I-HSA study was performed to measure the relative blood-pool distribution to correct the uptake of ^{123}I-2-iodo-L-phenylalanine in the tumor and the inflammation area as well as the rest of the animal for blood-pool activity. Ten tumor-bearing mice and 3 acute inflammation–bearing mice were injected with 7.4 MBq ^{123}I-HSA. Ten dynamic planar images of 1 min were acquired 10 min after injection. ROIs were drawn around the tumor or inflammation area and the contralateral background area. The tumor-to-contralateral background (RTB) and the inflammation-to-contralateral background (RIB) ratios were calculated and the mean for all animals was determined.

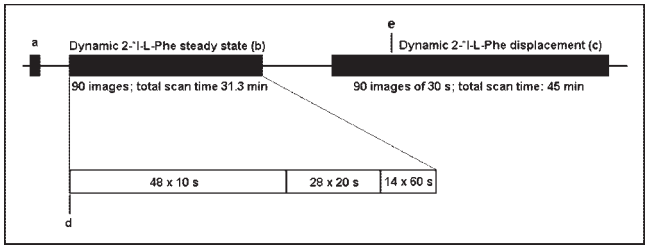

FIGURE 1. Scheme of planar imaging procedure. (a) Static acquisition to determine background radiation. (b) DPI to determine plateau phase (equilibrium) for ^{123}I-2-iodo-L-phenylalanine uptake. (c) DPI to determine displacement of ^{123}I-2-iodo-L-phenylalanine radioactivity with L-phenylalanine, L-methionine, or L-cysteine. (d) Injection of ^{123}I-2-iodo-L-phenylalanine at 0 min. (e) Injection of L-phenylalanine, L-methionine, or L-cysteine at 10 min.

The DPI experiments with ^{123}I-2-iodo-L-phenylalanine (Fig. 1) were started when the tumor reached a volume of 0.30 cm^3. Thirty tumor-bearing mice were followed-up with the new tracer until the tumor reached a volume of 5.00 cm^3.

DPI was started immediately after injection of 18.5 MBq ^{123}I-2-iodo-L-phenylalanine. First, the steady state of tracer uptake in the tumor was determined. Second, at steady state, a displacement study with L-phenylalanine, L-methionine, and L-cysteine—which all use the L-type transport system (*12*)—was performed. For the displacement study, 200 μL of a 145 mmol/L amino acid solution was intravenously injected in the lateral tail vein.

ROIs were drawn around the tumor, the contralateral background area, the right kidney, the heart, the pancreas, the brain, the thyroid, and the total body. In the case of the inflammation model, the ROI for the tumor was replaced by the ROI for the inflammation site. Due to superposition of the pancreas with other organs such as left kidney and stomach, the results will be overestimated, especially during the beginning of the DPI scan.

Tumor ^{123}I-2-iodo-L-phenylalanine uptake was compared with the uptake in the contralateral background area and the RTB was calculated. The significance of displacement of ^{123}I-2-iodo-L-phenylalanine activity by the 3 amino acids was calculated for a 95% confidence interval.

The ^{123}I-2-iodo-L-phenylalanine tumor uptake as a function of time, obtained from DPI experiments, were fit to a pseudo first-order model. The kinetic parameters half-life ($t_{1/2}$), time to reach equilibrium (t_R), and theoretic equilibrium for tumor tracer uptake were determined. The latter as well as the pseudo first-order fitting were performed in parallel with the in vitro experiments performed by Mertens et al. (*8*). The relationship of tumor volume as a function of t_R was examined, nonlinear regression was performed, and a theoretic rectangular hyperbole was calculated.

In the case of the inflammation model, the uptake of ^{123}I-2-iodo-L-phenylalanine in the inflammation area was compared with the contralateral background area and the RIB was calculated.

^{18}F-FDG Animal PET. PET was performed with a high-sensitivity animal PET scanner (VUB-PET; Vrije Universiteit Brussel; resolution, 3–4 mm) (*13*). Three NMRI mice bearing an acute inflammation and 3 R1M tumor–bearing athymic mice were injected with 18.5 MBq of ^{18}F-FDG. Fifteen minutes after injection, one time frame of 15 min was acquired. The images were reconstructed using Fourier rebinning and 2-dimensional order-subsets expectation maximization (*13*). The images produced had a matrix size of 128 × 128 × 19.

Volumes of interest (VOIs) were drawn around the tumor (or inflammation site) using an MR image. The VOI for the tumor was horizontally mirrored to create the contralateral background VOI. The values are expressed as counts per voxel and the RTB and RIB were calculated.

MRI. The tumor-bearing animals were anesthetized, and, after sedation, the animals were placed in a specially designed restrainer box in which sterile conditions could be retained. 3-Dimensional Dess-weighted images—hybrid T1–T2-weighted images—were generated on a 1-T whole-body system (Magnetom SP; Siemens) (*10*). The animals were scanned 2 at a time using a small surface flex coil.

Dissection: Biodistribution of ^{123}I-2-Iodo-L-Phenylalanine. The ID was calculated by weighing the syringes before and after injection of the tracer and by using a dilution series of the injected tracer solution that was also weighed and counted for radioactivity using the auto γ-counting system (CobraII Series; Canberra Packard).

Thirty R1M-bearing athymic mice were injected with 7.4 kBq ^{125}I-2-iodo-L-phenylalanine, 6 d after the last imaging experiment was performed. At various time points (2, 30, 45, 60, and 180 min) after injection, 6 animals per time point were sacrificed. The organs and tissues were removed, washed, and weighted. The blood was collected in an ethylenediaminetetraacetic acid (EDTA)-coated vial. The radioactivity of the samples was counted by use of an auto γ-counting system (CobraII Series). The amount of radioactivity in the organs and tissues was calculated as the differential absorption rate (DAR): $(\%ID/g)_{tumor}/(\%ID/g)_{total\ body}$.

Inflammation-bearing NMRI mice (n = 3) were injected with 7.4 kBq of ^{125}I-2-iodo-L-phenylalanine together with 16 MBq of ^{18}F-FDG through the lateral tail vein. After 30 min, the mice were sacrificed and organs and tissues were removed, washed, and weighted. Muscle tissue was collected from the inflamed left leg and the noninflamed right leg. The ^{18}F activity was counted on day 1 and the ^{125}I activity in the same samples was counted 3 d later. The amount of radioactivity in the organs and tissues was calculated as the DAR.

Metabolism Study: In Vivo Stability of ^{125}I-2-Iodo-L-Phenylalanine. The blood, collected in the tumor model biodistribution study, was used for a metabolism study of ^{125}I-2-iodo-L-phenylalanine as a function of time. Five hundred microliters of blood were centrifuged at 1,800*g* for 10 min, and the supernatant (plasma) was removed from the pellet. First, 200 μL of plasma were diluted 3 times with 9% NaCl. Second, 200 μL of this "plasma–NaCl solution" were added to the same volume of 20% trichloroacetic acid to denaturize the protein content. After a 5-min centrifugation at 1,800*g*, the supernatant was collected and filtered through a 0.22-μm filter. The samples were analyzed on RP-HPLC (C_{18} Hypersil BDS 5 μm; 250 × 46 mm; λ = 254 nm) (Alltech) with 20:80 MeOH/H_2O containing 1 mmol/L NH_4Ac (pH 5.5, 1 mL/min), and fractions of 0.5 mL were collected and counted by use of a γ-counting system (CobraII Series).

To determine the influence of EDTA on the formation of ^{125}I-2-iodo-L-phenylalanine metabolites, 2 control experiments were performed. First, 7.4 kBq of ^{125}I-2-iodo-L-phenylalanine were added to an EDTA-coated vial and treated identically to the blood

samples. Second, mouse blood was recovered from a wild-type NMRI mouse and 7.4 kBq of ^{125}I-2-iodo-L-phenylalanine were added. After 90 min of incubation at 37°C, the sample was treated as described earlier.

RESULTS

Synthesis and Radiolabeling of 2-I-L-Phenylalanine

Yields up to 65% were obtained for the presursor synthesis of 2-I-L-phenylalanine from 2-Br-L-phenylalanine using the Cu^{1+}-assisted nucleophilic exchange method.

Radioiodination of 2-I-L-phenylalanine by Cu^{1+}-assisted isotopic exchange, followed by Ag membrane filtration, resulted in a radiochemical purity of >99% and a specific activity of 65 GBq/mmol (^{123}I labeling) and 11 GBq/mmol (^{125}I labeling). In both cases, it was shown by chiral HPLC that there was no detectable amount of D analogs.

In Vivo Results

In Vivo Stability of ^{125}I-2-Iodo-L-Phenylalanine. HPLC analysis of the mouse blood showed a dehalogenation of 7.3% of ^{125}I-2-iodo-L-phenylalanine 90 min after injection. No other metabolites were detected. EDTA did not show any influence on the deiodination of ^{125}I-2-iodo-L-phenylalanine.

Planar Imaging. DPI with ^{123}I-HSA showed no significant difference between the blood flow in the tumor or inflammated muscle and the contralateral reference leg (RTB = 1.1 ± 0.2 and RIB = 1.1 ± 0.2).

The ^{123}I-2-iodo-L-phenylalanine uptake–time kinetics in R1M tumors in vivo is shown in Figure 2 and follows a rectangular hyperbolic shape. When plotting 1/(net tumor uptake) as a function of 1/time, a linear relationship ($R^2 >$ 0.95) is obtained (Fig. 3A). This means that important kinetic parameters such as $t_{1/2}$, velocity at initial conditions, and the theoretic equilibrium of tumor tracer uptake can be determined. This results in the calculated values for ^{123}I-2-iodo-L-phenylalanine of (net tumor uptake)$_{equilibrium}$ = 2.7 %ID/P and $t_{1/2}$ = 0.5 min. Figure 3B indicates that ^{123}I-2-iodo-L-phenylalanine uptake in R1M tumors follows a pseudo reversible first-order reaction ($R^2 > 0.90$) (*8*).

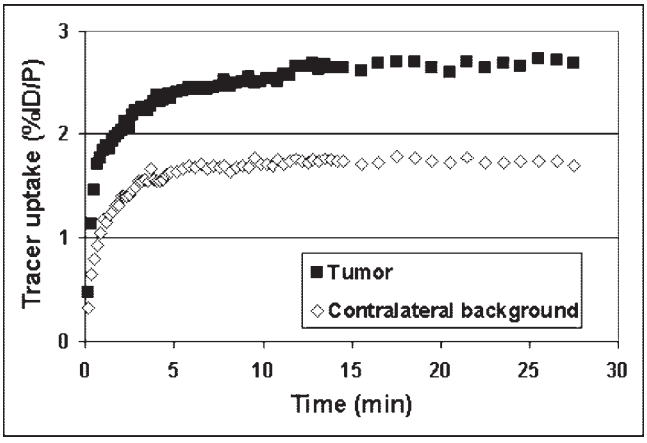

FIGURE 2. Overall mean uptake of ^{123}I-2-iodo-L-phenylalanine uptake (%ID/P) in tumor and contralateral background region as functions of time by DPI for tumor volumes ranging from 0.3 to 5.0 cm^3.

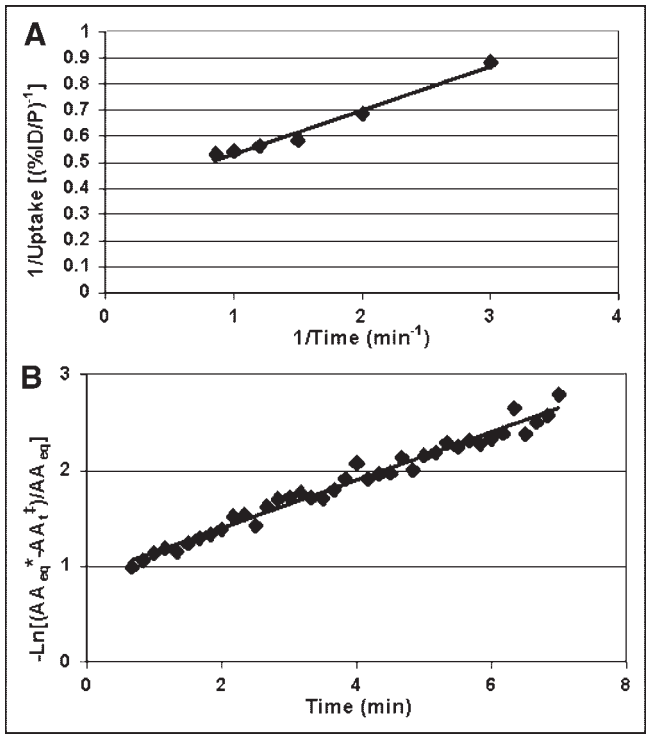

FIGURE 3. (A) Uptake of ^{123}I-2-iodo-L-phenylalanine: plot of $1/(AA_t)$ as function of 1/time. Equation of fitted curve: $y = 0.17x + 0.37$ ($R^2 = 0.9784$) resulting in $AA_{eq}^* = 2.73$ %ID/P and $t_{1/2} = 0.46$ min. (B) Uptake of ^{123}I-2-iodo-L-phenylalanine as function of time by DPI: pseudo first-order fit ($R^2 = 0.9764$). *Net ^{123}I-2-iodo-L-phenylalanine tumor uptake at equilibrium (%ID/P); ‡Net ^{123}I-2-iodo-L-phenylalanine tumor uptake when equilibrium is not reached (%ID/P).

At equilibrium (plateau phase), net ^{123}I-2-iodo-L-phenylalanine uptake in the tumor was high. It increased from 0.60 ± 0.03 %ID/P up to 5.7 ± 0.4 %ID/P for tumor volumes ranging from 0.3 to 5.0 cm^3 (Figs. 2 and 4A and 4B). When plotting the ^{123}I-2-iodo-L-phenylalanine tumor uptake at equilibrium as a function of tumor volume, we observed a large spread of the results ($R^2 = 0.11$) and no correlation between tumor uptake and tumor volume. When plotting the time to reach equilibrium, t_R, as a function of tumor volume, a hyperbolic curve ($R^2 > 0.90$) reaching a plateau up from a tumor volume of 4.0 cm^3 was obtained (Fig. 5). Nonlinear regression of a theoretic hyperbolic curve to the experimental values shows a top value of 15.3 ± 0.7 min. The experimental curve fitted the theoretic rectangular hyperbole ($R^2 = 0.91$) (Fig. 5).

The displacement of ^{123}I-2-iodo-L-phenylalanine activity in the tumor with L-phenylalanine, L-methionine, and L-cysteine is summarized in Table 1. The radioactivity in the tumor decreased rapidly for a small but significant amount

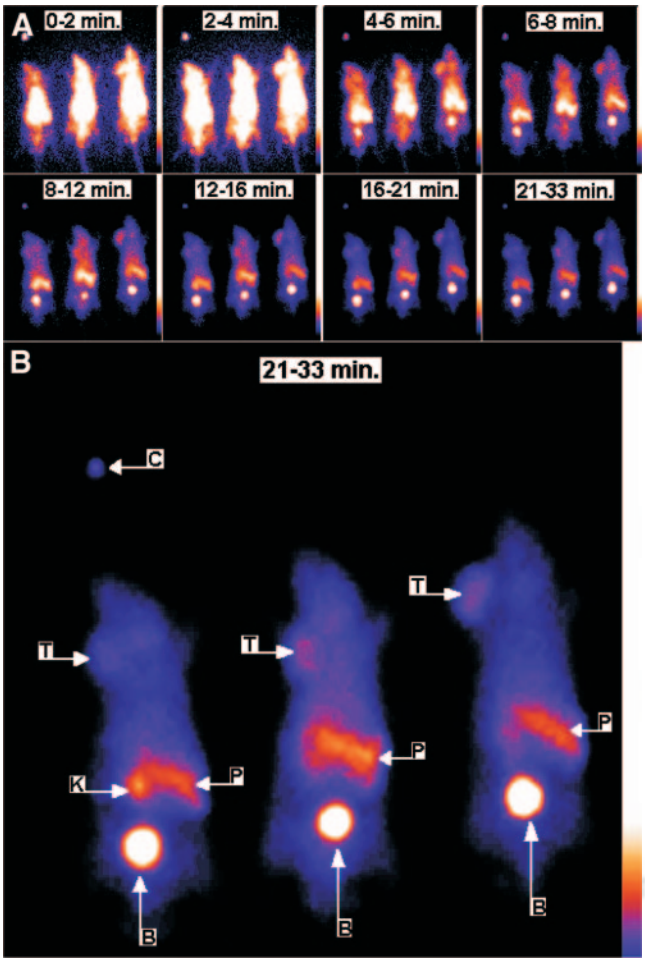

FIGURE 4. (A) Uptake of ^{123}I-2-iodo-L-phenylalanine uptake in the rhabdomyosarcoma tumor model as function of time by DPI for tumor volume of 0.50 cm^3. Each image is result of summation of 11 consecutive frames. Relative scaling was used (see colored tool bars) and each subpanel depicts 3 different animals for the time frame depicted at top of each subpanel. (B) Uptake of ^{123}I-2-iodo-L-phenylalanine at steady state. Panel depicts last time frame (subpanel) shown in A and shows 3 different animals for time frame of 21–33 min after tracer injection. B = bladder; P = pancreas zone; K = kidney; T = tumor; C = calibration syringe.

($P < 0.05$) after intravenous administration of those amino acids and reached a new plateau within 2 min.

^{123}I-2-Iodo-L-phenylalanine was cleared quickly through the kidneys, without accumulation, to the bladder (Fig. 6). This is confirmed by the fact that the first-order fits of the activity as a function of time were almost the same for kidneys and the heart (Fig. 6). High tracer uptake (3.3 ± 1.5 %ID/P) was noted in the zone of the pancreas but, due to superposition of the pancreas with other organs such as the left kidney and the stomach, the results are overestimated (*14*). Low uptake of radioactivity in the thyroid (2.1 ± 1.1 %ID/P), brain (1.5 ± 0.8 %ID/P), or abdominal organs was observed (Fig. 7).

There was no significant (detectable) increased uptake of

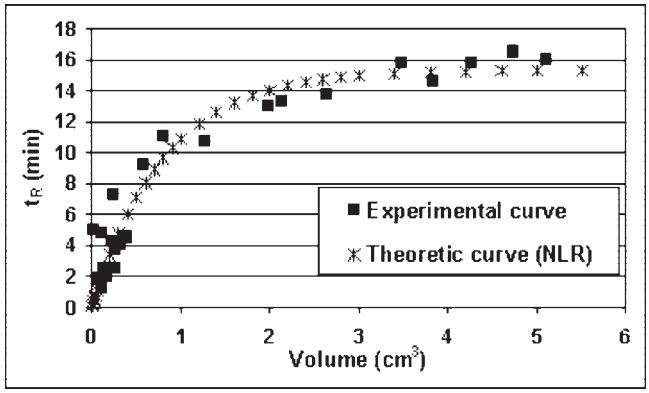

FIGURE 5. Time to reach equilibrium (t_R) as function of tumor volume. NLR = nonlinear regression.

^{123}I-2-iodo-L-phenylalanine in the inflammation area. The RIB was 0.97 ± 0.14. This results in an apparent tumor–to–inflamed tissue ratio (T/I ratio) of 5.9 ± 0.42.

^{18}F-FDG Animal PET. The uptake of ^{18}F-FDG was high in the tumor and also in the inflammation area. A RTB of 3.6 ± 1.6 and a RIB of 2.3 ± 0.6 were obtained. The resulting apparent T/I ratio is 1.6 ± 1.2.

Biodistribution by Dissection. The biodistribution data of ^{125}I-2-iodo-L-phenylalanine in R1M tumor–bearing athymic mice are shown in Table 2.

The net ^{125}I-2-iodo-L-phenylalanine tumor uptake reached equilibrium up from 60 min with a mean DAR of 3.8 ± 1.5. At the same time point, ^{125}I-2-iodo-L-phenylalanine activity in the blood and in the contralateral leg tissue reached a DAR of 1.1 ± 0.3 and 0.6 ± 0.2, respectively.

^{125}I-2-Iodo-L-phenylalanine was cleared very fast through the kidneys, without accumulation, to the bladder. A significant uptake of radioactivity in the pancreas was observed. No significant accumulation of radioactivity was observed in other abdominal organs, such as liver, lungs, small intestine, and large intestine, or in the brain.

TABLE 1
Displacement Study of ^{123}I-2-Iodo-L-Phenylalanine Activity in Tumor Using Planar γ-Scintigraphy

Amino acid	Contribution of transport systems (%)	%P*	%D†
L-Phenylalanine	L (70), ASC (25), O (5)	72	12.3 ± 4.2
L-Methionine	L (50), ASC (20), A (10), O (20)	80	16.0 ± 4.2
L-Cysteine	L (30), ASC (55), A (10), O (5)	57	11.5 ± 7.8

*Percentage of all animals in which significant displacement of radioactivity was observed (n = 25).

†Percentage of tracer decrease by administering the amino acid (mean ± SD).

L = L-type transporter system; ASC = alanine, serine, and cysteine–type transporter system; O = other transporter systems; A = A-type transporter system.

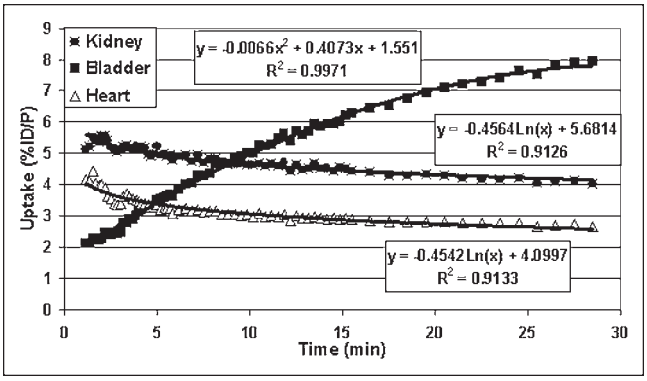

FIGURE 6. Uptake of ^{123}I-2-iodo-L-phenylalanine uptake (%ID/P) as function of time by DPI: clearance of tracer through kidneys to bladder.

The biodistribution data of ^{125}I-2-iodo-L-phenylalanine and ^{18}F-FDG in inflammation-bearing NMRI mice are shown in Table 3. A marked high ^{18}F-FDG uptake in the inflamed muscle with a RIB value of 11.1 ± 1.7 is observed, whereas only a small increase of ^{125}I-2-iodo-L-phenylalanine uptake in the inflammation site vis à vis the contralateral muscle was noticed with a RIB value of 1.30 ± 0.02. This results in a ratio T/I of 8.5 ± 1.7.

The discrepancies between results obtained by DPI and the dissection could not only be explained by biodiversity but could also be due to the well-known differences in resolution and counts acquisition between the methods used.

DISCUSSION

2-Iodo-L-phenylalanine was developed as an alternative SPECT tumor tracer to 4-iodo-L-phenylalanine, 2-iodo-L-tyrosine, and 3-iodo-α-methyltyrosine to overcome the high blood-pool and inflammation activity, the difficult precursor synthesis, and the marked long-term renal accumulation, respectively (*15–17*).

Cu^{1+}-Assisted nucleophilic exchange provides not only an easy 1-step reaction for precursor synthesis but also the possibility to establish a kit formulation for fast and quantitative routine radioiodination of 2-I-L-phenylalanine without the need of an extra purification procedure.

In vitro in R1M cells, the uptake kinetics and the Michaelis–Menten constant values of ^{125}I-2-iodo-L-phenylalanine and the natural amino acid L-phenylalanine are both similar and both amino acids are transported by the obligatory exchange LAT1 system. Moreover, our research group revealed that ^{125}I-2-iodo-L-phenylalanine is not incorporated into the cell proteins and that the uptake of the tracer at equilibrium reflects the total "amino acid turnover" of the R1M tumor cells. Recent evidence verified that incorporation of radiolabeled amino acids is not necessary for tumor imaging and that the increased uptake is directly related to the metabolic requirement of the tumor cells (*8*).

With regard to these characteristics, the new tracer $^{123/125}$I-2-iodo-L-phenylalanine, which has a free para position and is somewhat less lipophilic than 4-iodo-L-phenylalanine, was evaluated in vivo in view of its potential application for oncologic imaging with SPECT.

The planar imaging experiments with the new tracer showed that the same uptake kinetics, compared with the in vitro experiments, could be applied: The uptake as a function of time followed a rectangular hyperbolic curve and Figure 3B indicated that for the uptake a pseudo reversible, pseudo first-order reaction was followed (*8*). These observations strongly suggest that, in vivo, $^{123/1225}$I-2-iodo-L-phenylalanine is also transported by the LAT1 system.

The latter hypothesis is confirmed by the displacement study. Although the displaced ^{123}I-2-iodo-L-phenylalanine radioactivity in the tumor by L-phenylalanine, L-methionine, and L-cysteine was small, it was significant (Table 1). This shows that the transporter system involved is of the "obligatory exchanger" type, such as LAT1. The rather small amount of displaced radioactivity can be explained by the fact that the blood plasma is continuously filtered in the kidneys by the glomerulus and the Bowman's capsule. When a huge excess of amino acids, such as L-phenylalanine and L-methionine, is administered to the animals, the excess will be immediately excreted to the urinary tractus.

$^{123/125}$I-2-Iodo-L-phenylalanine accumulated quickly to reach high amounts in the R1M tumors, and only a very small part showed dehalogenation after 90 min (Fig. 5; Table 2). Moreover, low abdominal background, fast blood clearance, low brain uptake, and almost negligible uptake in inflammatory tissue (T/I ratios of 1.3 and 1.6), in comparison with ^{18}F-FDG (T/I ratios of 5.9 and 8.5), were observed. These findings are also confirmed in the literature for another radiolabeled amino acid, 2-iodo-L-tyrosine, which showed a much lower uptake in the site of inflammation in comparison with ^{18}F-FDG (*17*).

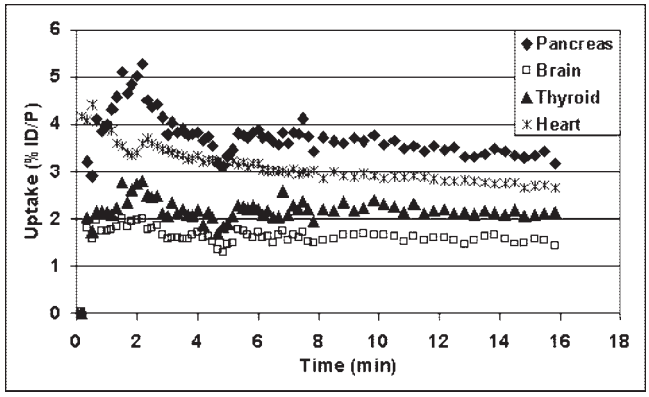

FIGURE 7. Uptake of ^{123}I-2-iodo-L-phenylalanine uptake (%ID/P) in heart, pancreas, brain, and thyroid as function of time by DPI.

TABLE 2
Biodistribution Study by Dissection of ^{123}I-2-Iodo-L-Phenylalanine in R1M-Bearing Athymic Mice (n = 6)

Tissue	DAR (mean ± SD)				
	2 min	30 min	45 min	60 min	180 min
Blood	1.76 ± 0.94	1.46 ± 0.37	1.39 ± 0.28	1.06 ± 0.31	1.16 ± 0.21
Brain	0.34 ± 0.01	0.49 ± 0.09	0.55 ± 0.18	0.63 ± 0.16	0.47 ± 0.07
Heart	1.31 ± 0.15	0.84 ± 0.23	0.65 ± 0.09	0.82 ± 0.04	0.74 ± 0.18
Lung	1.33 ± 0.28	1.11 ± 0.50	0.69 ± 0.24	0.80 ± 0.07	0.86 ± 0.25
Stomach	0.88 ± 0.20	1.98 ± 1.23	2.60 ± 1.25	3.34 ± 0.24	2.61 ± 1.59
Liver	0.88 ± 0.08	0.52 ± 0.17	0.42 ± 0.08	0.53 ± 0.08	0.56 ± 0.10
Kidneys	4.81 ± 2.16	1.73 ± 0.51	1.79 ± 0.46	1.45 ± 0.10	1.03 ± 0.28
Small intestine	0.57 ± 0.05	0.61 ± 0.08	0.59 ± 0.20	0.76 ± 0.12	0.70 ± 0.23
Large intestine	0.41 ± 0.13	0.29 ± 0.03	0.18 ± 0.07	0.32 ± 0.08	0.44 ± 0.13
Pancreas	5.37 ± 1.03	4.71 ± 1.00	4.56 ± 1.98	7.87 ± 2.61	8.64 ± 1.74
Front leg	0.77 ± 0.23	0.43 ± 0.38	0.64 ± 0.36	0.56 ± 0.24	0.47 ± 0.12
Tumor	1.13 ± 0.11	2.58 ± 0.61	2.70 ± 0.23	3.76 ± 0.52	3.02 ± 0.39
RTB	1.61 ± 0.72	3.58 ± 0.97	5.02 ± 2.20	6.71 ± 1.26	6.35 ± 1.05

DAR was calculated at various time points after injection.

Just like ^{123}I-2-iodo-L-tyrosine, ^{123}I-4-iodo-L-phenylalanine, and ^{123}I-3-iodo-α-methyltyrosine uptake in rodents (*17,18*), ^{125}I-2-iodo-L-phenylalanine showed high uptake in the pancreas. This is typical for labeled amino acid analogs in rodents. In patients, no significant pancreatic uptake was observed for 2-iodo-L-tyrosine and ^{123}I-3-iodo-α-methyltyrosine (*15,17*).

The relationship between the time to reach the steady state for ^{123}I-2-iodo-L-phenylalanine tumor uptake in vivo and the tumor volume reached a plateau phase at a tumor volume of 4 cm^3, which could be due to the higher level of necrosis in the larger tumors. It was shown that, even when the radiolabeled synthetic amino acid tumor tracer is not incorporated into cell proteins, the uptake reflects the total amino acid turnover of the tumor cells (*8*).

TABLE 3
Biodistribution Study by Dissection of ^{125}I-2-Iodo-L-Phenylalanine and ^{18}F-FDG in NMRI Mice Bearing Inflammation (n = 3)

Tissue	DAR (mean ± SD)	
	^{18}F-FDG	^{125}I-L-2-Phenylalanine
Blood	0.92 ± 0.09	1.10 ± 0.11
Brain	2.10 ± 0.17	0.57 ± 0.20
Heart	0.50 ± 0.28	1.00 ± 0.10
Lung	0.61 ± 0.28	0.80 ± 0.15
Stomach	0.88 ± 0.25	0.29 ± 0.16
Liver	0.37 ± 0.20	0.42 ± 0.53
Kidneys	1.92 ± 1.14	1.92 ± 0.37
Small intestine	0.34 ± 0.05	0.68 ± 0.19
Large intestine	0.17 ± 0.10	0.36 ± 0.09
Pancreas	3.51 ± 1.03	4.22 ± 1.30
Muscle	1.85 ± 0.01	0.65 ± 0.07
Inflamed muscle	20.50 ± 3.30	0.84 ± 0.10
Inflammation/muscle ratio	11.06 ± 1.72	1.29 ± 0.02

CONCLUSION

^{123}I-2-Iodo-L-phenylalanine is a promising tracer for intracranial as well as extracranial oncologic imaging with SPECT because of its high and fast tumor accumulation, low renal and brain uptake, and minor accumulation in acute inflammatory lesions. Furthermore, its chemical synthesis is easy and allows a kit formulation, which is a benefit for transferring the tracer to clinical use.

ACKNOWLEDGMENT

Financial support was given by the Fonds voor Wetenschappelijk Onderzoek.

REFERENCES

1. Yanagida O, Kanai Y, Chairoungdua A, et al. Human L-type amino acid transport system 1 (LAT1): characterisation of function and expression in tumour cell lines. *Biochim Biophys Acta.* 2001;1514:291–302.
2. Jager PL, Vaalburg W, Pruim J, et al. Radiolabelled amino acids: basic aspects and clinical applications in oncology. *J Nucl Med.* 2001;42:432–445.
3. Weber W, Bartenstein P, Gross MW, et al. Fluorine-18-FDG PET and iodine-123-IMT SPECT in the evaluation of brain tumors. *J Nucl Med.* 1997;38:802–808.
4. Langen KJ, Ziemons K, Kiwit JC, et al. 3-[^{123}I]Iodo-alpha-methyltyrosine and [methyl-^{11}C]-L-methionine uptake in cerebral gliomas: a comparative study using SPECT and PET. *J Nucl Med.* 1997;38:517–522.
5. Kubota K, Yamada S, Kubota R, et al. Intramural distribution of fluorine-18-fluorodeoxyglucose in vivo: high accumulation in macrophages and granulation tissues studied by microautoradiography. *J Nucl Med.* 1992;33:1972–1980.
6. Mertens JR, Lahoutte T, Joos C, et al. In vivo evaluation of 2-^{123}I-Tyr and 2-^{123}I-Phe as tumour specific tracers for SPECT [abstract]. *Eur J Nucl Med.* 2002;29:S76.
7. Samnick S, Schaefer A, Siebert S, et al. Preparation and investigation of tumor affinity, uptake kinetic and transport mechanism of iodine-123-labelled amino acid derivatives in human pancreatic carcinoma and glioblastoma cells. *Nucl Med Biol.* 2001;28:13–23.

8. Mertens JR, Lahoutte T, Joos C, et al. New approach of cell uptake kinetics of L-2-^{123}I-Tyr and L-2-^{123}I-Phe, new potential tumour tracers for SPECT [abstract]. *Eur J Nucl Med.* 2002;29:S377.
9. Mertens J, Gysemans M. Cu^{1+}-Assisted nucleophilic exchange radiohalogenation: application and mechanistic approach. In: Ali M, Emran AM, eds. *New Trends In Radiopharmaceutical Synthesis, Quality Assurance And Regulatory Control.* New York, NY: Plenum Press; 1991:53–65.
10. Waterton JC, Alott CP, Pickfort R, et al. Assessment of mouse tumour xenograft volumes in vivo by ultrasound imaging, MRI and calliper measurement. In: Faulkner K, Carey B, Crellin A, Harisson RM, eds. *Proceedings of the 19th LH Gray Conference: Quantitative Imaging in Oncology.* London, U.K.: Kluwer Academic Publishers; 1997:146–149.
11. Hoffman AJ, Huang SC, Phelps ME. Quantitation in positron emission computed tomography. 1. Effect of object size. *J Comput Assist Tomogr.* 1979;3:299–308.
12. Christensen NC. Role of amino acid transport and countertransport in nutrition and metabolism. *Phys Rev.* 1990;70:43–77.
13. Xuan L, Rajeswaran S, Smolik W, et al. Design and physical characteristics of a small animal PET using BaF2 crystals and a photosensitive wire chamber. *Nucl Instr Methods.* 1996;A382:589–600.
14. Cook, MJ. *The Anatomy of the Laboratory Mouse.* New York, NY: Academic Press; 1965:55–78.
15. Langen KJ, Pauleit D, Coenen HH. 3-[^{123}I]Iodo-alpha-methyl-L-tyrosine: uptake mechanisms and clinical applications. *Nucl Med Biol.* 2002;29:625–631.
16. Jager PL, Franssen EJ, Kool W, et al. Feasibility of tumor imaging using L-3-[iodine-123]-iodo-alpha-methyl-tyrosine in extracranial tumors. *J Nucl Med.* 1998;39:1736–1743.
17. Lahoutte T, Mertens J, Caveliers V, et al. Comparative biodistribution of iodinated amino acids in rats: selection of the optimal analog for oncologic imaging outside the brain. *J Nucl Med.* 2003;44:1489–1494.
18. Vekeman M, Chavatte K, Lahoutte T, et al. L-[2-Radioiodo]tyrosine, a new potential protein synthesis and tumour tracer for spect: radiosynthesis and biodistribution in rodent [abstract]. *Eur J Nucl Med.* 1999;26:S43.